

Disturbance Rejection and Asymptotically Stabilizing Control for a Quadrotor UAV

Runxia Guo *, Jiankang Dong *, Yi Zhu **

* College of Aeronautical Automation, Civil Aviation University of China, Tianjin, China, (e-mail: rxguoblp@163.com, jkdong@cauc.edu.cn)

** College of Flight Technology, Civil Aviation University of China, Tianjin, China, (e-mail: yzhu@cauc.edu.cn)

Abstract: A novel attitude controller based on Lyapunov stability theory is developed for a quadrotor UAV considering different bounded disturbances and parameters' perturbation. Specifically, the proposed controller is able to compensate for a disturbance without requiring concrete information of its structure (e.g. period or amplitude). In addition, the controller can handle the situation when external disturbances and internal parameters' perturbation exist simultaneously. Furthermore, sufficient conditions are derived for the control law to ensure asymptotic stability of the closed loop system. A theoretically rigorous proof has been given. Numerical simulations are carried out to evaluate the effectiveness of the control algorithm. Simulation results show that the proposed control strategy has a satisfactory performance in both disturbance rejection and anti-multi-parameter perturbation.

Keywords: Quadrotor UAV, Attitude Control, Asymptotic Stability, Disturbance Rejection, Anti-multi-parameter Perturbation

1. INTRODUCTION

Quadrotor Unmanned Aerial Vehicle (UAV) have obtained considerable development in the last two decades in view of their large variety of application and the fact that they are easily transportable and maneuverable. However, the quadrotor UAV suffer from various control complexities such as: 1) Weak anti-jamming capability; 2) Parameters' perturbation within the system model; 3) Underactuated characteristic; 4) Open-loop instability.

In response to these difficulties, researchers have employed various modeling and control development techniques to solve aspects 1)–3). For example, the attitude control of a quadrotor aircraft subject to a class of time varying and non-vanished disturbances was studied in (Zhang et al., 2010). An observer was designed to estimate disturbances. Based on the estimation, a feedback controller with a sliding mode term was designed to stabilise the attitude of the quadrotor. The designed continuous feedback controller made the attitude error uniformly ultimate bounded. Theoretical results were confirmed by numerical simulations. For the parameters' perturbation problem, a robust adaptive controller on $SO(3)$ was developed (Lee, 2013) to track the attitude and angular velocity command without the knowledge of the inertia matrix of a rigid body. An estimate of the inertia matrix was updated online to provide an asymptotic tracking property when the inertia matrix was not available. These characteristics were illustrated by the experimental results of the attitude dynamics of a quadrotor UAV. For the underactuated question, the fuzzy logic control and sliding mode control techniques based on backstepping approach

were integrated to develop a robust fuzzy backstepping sliding mode controller (RFBSMC) for an under-actuated quadrotor UAV system under external disturbances and parameter uncertainties (Khebbache and Tadjine, 2013; Xu and Ozguner, 2008). In addition, in order to solve the problem of inherent nonlinearities in dynamics model, an efficient Model Predictive Control (eMPC) algorithm deploying fewer prediction points and requiring less computation was presented in (Abdolhosseini et al., 2013, 2012; Kutay et al., 2005). A model reduction technique associated with the dynamics of a quadrotor UAV was also put forward so as to minimize the burden of calculations in application of MPC into an airborne platform. Recently, a nonlinear optimal and suboptimal control technique based on control Lyapunov functions (CLF) was developed to achieve the goal of energy saving (Santos et al., 2013; Nagaty et al., 2013; Srinivasan et al., 2009).

In this paper, the topics of disturbance rejection and anti-multi-parameter perturbation are further pursued by designing a novel nonlinear saturated controller that is capable of compensating for external aperiodic bounded disturbances and internal parameters' perturbation.

The main contribution of this paper lies in three aspects: firstly, the designed controller is able to compensate for a disturbance without requiring the concrete information of its structure (e.g. period or amplitude); secondly, the controller can handle the situation when external disturbances and internal parameters' perturbation exist simultaneously; thirdly, the design of controller is based on analytical models with a theoretically rigorous proof, rather than intelligent

methods (for example, fuzzy logic control). All these three aspects of research work are not perfect in the existing literature.

The structure of this paper is organized as follows. The dynamics model of a quadrotor UAV is presented in section 2. Section 3 identifies the control objectives and constraints under which the controller is developed. An estimation algorithm for external disturbances and a saturated control force input are designed respectively in section 4. A Lyapunov stability analysis is utilized to illustrate the asymptotically stabilizing regulation for the pitch channel. Simulation results are presented in section 5. Conclusions and future works are discussed in section 6.

2. SYSTEM MODEL

The quadrotor UAV selected in this paper contains four rotors. In order to produce rotational torque, the quadrotor should change the rotational speed of the corresponding rotors. For example, when the 2nd rotor's rotational speed increases and the 4th rotor's rotational speed reduces at the same time, the quadrotor will yield (shown in Fig.1).

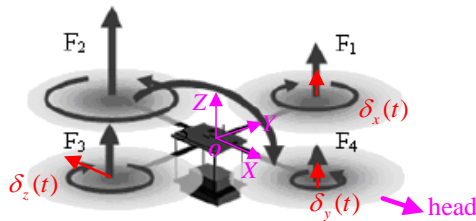


Fig. 1. Dynamics model of selected quadrotor UAV.

In Fig.1, F_1, F_2, F_3 and F_4 denote the corresponding rotor's lift respectively, O denotes the quadrotor's gravity center in body coordinate system, X, Y and Z respectively denote roll axis, pitch axis and yaw axis in body coordinate system, δ_x, δ_y and $\delta_z \in \mathfrak{R}^1$ denote the disturbance forces that are equivalent to the gravity center on the corresponding axis.

In order to simplify the mathematical model of quadrotor UAV, the following assumptions need to be taken into account:

- 1) Taking the quadrotor UAV as a rigid body, ignoring the influence of elasticity, and the quality and its distribution are invariant.
- 2) The earth is treated as a static plane.
- 3) Assuming OXZ plane and OYZ plane are two symmetrical planes in body coordinate system, which means the product of inertia $I_{XY, YZ, XZ} = 0$.
- 4) Assuming the acceleration of gravity does not change with altitude.

According to Newtonian mechanics, when a rigid body rotates around a fixed axis, the relationship between its

angular acceleration and rotational torque can be expressed as:

$$\dot{\omega} = M / I \quad (1)$$

where $\omega \in \mathfrak{R}^1$ represents the angular speed, $M \in \mathfrak{R}^1$ represents the rotational torque, $I \in \mathfrak{R}^1$ denotes the moment of inertia on corresponding axis.

Combining assumptions 1) ~ 4) above and the Newtonian mechanics equation (1), the 3-DOF orientation of quadrotor UAV can be modeled in body coordinate system as following:

$$\begin{cases} \ddot{\theta} = l(F_2 - F_4 - \eta_1 \dot{\theta} + \delta_y(t)) / I_y \\ \ddot{\phi} = l(F_1 - F_3 - \eta_2 \dot{\phi} + \delta_x(t)) / I_x \\ \ddot{\psi} = [C(F_2 + F_4 - F_1 - F_3) - \eta_3 \dot{\psi} + l\delta_z(t)] / I_z \end{cases} \quad (2)$$

where θ, ϕ and $\psi \in \mathfrak{R}^1$ represent real-time pitch, roll and yaw respectively, l represents the arm length from the gravity center to each rotor's axis, I_x, I_y and $I_z \in \mathfrak{R}^1$ denote the moment of inertia on the corresponding axis, η_1, η_2 and $\eta_3 \in \mathfrak{R}^1$ denote resistance coefficients, C denotes the proportional coefficient of the lift to the rotational torque.

The control force inputs are selected as (3).

$$\begin{cases} u_1 = F_2 - F_4 \\ u_2 = F_1 - F_3 \\ u_3 = F_2 + F_4 - F_1 - F_3 \end{cases} \quad (3)$$

where u_1, u_2 and $u_3 \in \mathfrak{R}^1$ denote synthesized control force inputs of pitch, roll and yaw respectively.

Therefore, the dynamics model can be re-written as:

$$\begin{cases} \ddot{\theta} = \frac{l}{I_y} u_1 - \frac{l \cdot \eta_1}{I_y} \dot{\theta} + \frac{l}{I_y} \delta_y(t) \\ \ddot{\phi} = \frac{l}{I_x} u_2 - \frac{l \cdot \eta_2}{I_x} \dot{\phi} + \frac{l}{I_x} \delta_x(t) \\ \ddot{\psi} = \frac{C}{I_z} u_3 - \frac{\eta_3}{I_z} \dot{\psi} + \frac{l}{I_z} \delta_z(t) \end{cases} \quad (4)$$

Remark 1: From (4), it is clear that pitch, roll and yaw have same forms. Therefore, the following designed controller combined with necessary parameters' modification will be equally applicable to the attitude control of roll and yaw.

To simplify writing and reading, the pitch dynamics model is re-written as (5).

$$\ddot{\theta} = c_1 u - c_2 \dot{\theta} + c_1 \delta(t) \quad (5)$$

where $c_1 = \frac{l}{I_y}, c_2 = \frac{l \cdot \eta_1}{I_y}, \delta(t) = \delta_y(t)$.

When there is no disturbance $\delta(t)$, (5) can be simplified as the following nominal model:

$$\ddot{\theta} = c_1 u - c_2 \dot{\theta} \tag{6}$$

3. PROBLEM STATEMENT

The objective of the design process is to specify a control force input signal that will regulate the pitch angle to a desired value while the quadrotor UAV is being subjected to unknown external disturbances (e.g. the wind disturbance) or internal parameters' perturbation.

The design process is complicated due to the common fact that the quadrotor is open-loop unstable and the lack of knowledge of disturbances. In order to facilitate the control development, the target pitch tracking error signal $e(t) \in \mathfrak{R}^1$ and the filtered tracking error signal $r(t) \in \mathfrak{R}^1$ are defined in the following manner:

$$e = \theta - \theta_d \tag{7}$$

$$r = \dot{e} + \alpha e \tag{8}$$

where $\theta_d \in \mathfrak{R}^1$ denotes a desired pitch angle and $\alpha \in \mathfrak{R}^1$ represents a positive, constant control gain. The proposed control strategy is developed under the assumption that the pitch angle and angular velocity signals are available for the measurement.

Remark 2: $r(t)$ in (8) evaluates comprehensively the tracking error itself and the first order derivative of the tracking error. The first derivative of error representing the rate of change has a significant impact on the dynamic performance

of the closed loop control system (e.g. when $\|\dot{e}\|$ is too large, it may induce a high-frequency oscillation in the dynamic adjustment process, even though the system remains final closed-loop stable.). Therefore, the designed control law based on $r(t)$ in (8) can meet the requirements of both dynamic and static performances, rather than just guaranteeing the system closed-loop stable.

4. DESIGN OF CONTROLLER

The development of controller is simplified by rewriting the second-order system (5) in terms of filtered tracking error signal $e(t)$ and $r(t)$ in the following manner:

$$\dot{r} = c_1 u + (\alpha - c_2)(r - \alpha e) + c_1 \delta(t) \tag{9}$$

Based on the structure of ensuing stability analysis, the control force input u is designed in the following manner:

$$u = -\frac{k_2}{c_1} \tanh(k_1 r) - 4 \tanh(k_1 r) \delta_0^2 - 2 \operatorname{sgn}(r) \delta_0 - \hat{\delta}(t) \tag{10}$$

where $k_1, k_2 \in \mathfrak{R}^1$ represent positive constants, $\hat{\delta}(t) \in \mathfrak{R}^1$

represents an estimation for $\delta(t)$, $\delta_0 \in \mathfrak{R}^1$ is a positive constant that represents the maximum acceptable disturbance force, $\operatorname{sgn}(\bullet)$ is the standard signum function.

After substituting the control input (10) into open loop dynamics (9), the closed loop dynamics for $e(t)$ and $r(t)$ can be formulated as:

$$\begin{aligned} \dot{r} = & -k_2 \tanh(k_1 r) + (\alpha - c_2)(r - \alpha e) \\ & + (c_1 \delta(t) - c_1 \hat{\delta}(t) - 2c_1 \operatorname{sgn}(r) \delta_0 - 4c_1 \tanh(k_1 r) \delta_0^2) \end{aligned} \tag{11}$$

4.1 Disturbances Estimation

The control input (10) contains the estimation information of unknown disturbances. Here, the model reference adaptive method is used to develop the estimator.

The output of the actual pitch in (5) subtracts the desired output in nominal model (6), and the following expression is obtained:

$$\ddot{\varepsilon} = -c_2 \dot{\varepsilon} + c_1 \tilde{\delta}(t) \tag{12}$$

where $\tilde{\delta}(t) \in \mathfrak{R}^1$ represents the preliminary estimation of disturbance $\delta(t)$, $\varepsilon \in \mathfrak{R}^1$ represents the deviation between the actual output and the desired output. Its value is equal to $(\theta - \theta_d)$, θ_d is the output of nominal model (6).

From (12), the value of $\tilde{\delta}(t)$ is obtained:

$$\tilde{\delta}(t) = (\ddot{\varepsilon} + c_2 \dot{\varepsilon}) / c_1 \tag{13}$$

In (13), the preliminary estimation $\tilde{\delta}(t)$ requires the knowledge of the first and second order derivative of the error in controller response. This error term can itself be noisy due to the errors in disturbance and parameter identification. The second order derivative of the error term will be even noisier. As such, the saturation limiter is necessary and an estimator for $\delta(t)$ is generated online via the following expression:

$$\hat{\delta}(t) = \begin{cases} (\ddot{\varepsilon} + c_2 \dot{\varepsilon}) / c_1 & |(\ddot{\varepsilon} + c_2 \dot{\varepsilon}) / c_1| < \delta_0 \\ \operatorname{sgn}(\ddot{\varepsilon} + c_2 \dot{\varepsilon}) \cdot \delta_0 & |(\ddot{\varepsilon} + c_2 \dot{\varepsilon}) / c_1| \geq \delta_0 \end{cases} \tag{14}$$

The schematic diagram of disturbance estimation is shown in Fig.2.

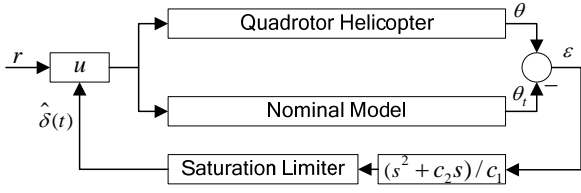


Fig. 2. Schematics of disturbances estimation $\hat{\delta}(t)$.

Remark 3: In fact, $\hat{\delta}(t)$ in expression (14) considers errors caused by internal parameters' perturbation in addition to external disturbances. Because both the internal parameters' perturbation and the external disturbances may cause deviation between the actual output θ (θ contains errors caused by internal parameters' perturbation) and the expected output θ_i (θ_i doesn't contain errors caused by internal parameters' perturbation). This deviation that is $\varepsilon = (\theta - \theta_i)$ has been included in $\hat{\delta}(t)$ (see (14)), in other words, the errors caused by internal parameters' perturbation have also been taken into account by $\hat{\delta}(t)$.

Therefore, the designed control law (10) based on $\hat{\delta}(t)$ in expression (14) can handle the situation when the internal parameters' perturbation exists. The subsequent simulation experiment 2 will illustrate it. In addition, the saturation limiter has taken into account the actual anti-jamming capability of the quadrotor. Therefore, this estimation approach is consistent with the actual situation.

4.2 Asymptotically Stabilizing Controller Design

Theorem: If the control gains are selected to satisfy the condition:

$$2\alpha \frac{k_2}{c_1} - \left[\frac{\alpha - c_2}{c_1} \right]^2 \alpha^2 > [|\dot{e}(0)| + \alpha |e(0)| + \frac{1}{2} c_1 |e(0)|^2 + \frac{1}{k_1} (1 + \ln 2)]^2 \quad (15)$$

where $e(0)$ and $\dot{e}(0)$ denote the initial pitch angle/angular velocity tracking error in (5), then the control input (10) can ensure that the pitch tracking error $e(t)$ is driven asymptotically to zero, in the sense that:

$$\lim_{t \rightarrow \infty} e(t) = 0 \quad (16)$$

Proof: A Lyapunov function $V(t)$ is defined as:

$$V(t) = \frac{1}{k_1 c_1} \ln(\cosh(k_1 r)) + \frac{1}{2} e^2 + \int_0^t \{ [\delta(\sigma) - \hat{\delta}(\sigma)]^2 \tanh^2(k_1 r) \} d\sigma \quad (17)$$

Remark 4: $V(t)$ evaluates comprehensively the characteristics of the filtered tracking error signal $r(t)$, tracking error signal $e(t)$ and the estimation error $[\delta(t) - \hat{\delta}(t)]$.

After taking the time derivative of (17) and substituting (7), (8) and (11) into it, the following expression is obtained:

$$\begin{aligned} \dot{V} &= \frac{1}{c_1} \tanh(k_1 r) \dot{r} + e \dot{e} + [\delta(t) - \hat{\delta}(t)]^2 \tanh^2(k_1 r) \\ &= \frac{1}{c_1} \tanh(k_1 r) [-k_2 \tanh(k_1 r) + (\alpha - c_2)(r - \alpha e) \\ &\quad + (c_1 \delta(t) - c_1 \hat{\delta}(t) - 2c_1 \operatorname{sgn}(r) \delta_0 - 4c_1 \tanh(k_1 r) \delta_0^2)] \\ &\quad + e(r - \alpha e) + [\delta(t) - \hat{\delta}(t)]^2 \tanh^2(k_1 r) \\ &= \frac{1}{c_1} \tanh(k_1 r) [-k_2 \tanh(k_1 r) + (\alpha - c_2)(r - \alpha e)] + e(r - \alpha e) \\ &\quad + \frac{1}{c_1} \tanh(k_1 r) [(c_1 \delta(t) - c_1 \hat{\delta}(t) - 2c_1 \operatorname{sgn}(r) \delta_0 \\ &\quad - 4c_1 \tanh(k_1 r) \delta_0^2)] + [\delta(t) - \hat{\delta}(t)]^2 \tanh^2(k_1 r) \\ &= \left[-\frac{k_2}{c_1} + \frac{(\alpha - c_2)r}{c_1 \tanh(k_1 r)} \right] \tanh^2(k_1 r) \\ &\quad - \underbrace{e \tanh(k_1 r) \left[\frac{\alpha(\alpha - c_2)}{c_1} - \frac{r}{\tanh(k_1 r)} \right]}_{\text{term1}} - \alpha e^2 \\ &\quad + \underbrace{\tanh(k_1 r) [c_1 \delta(t) - c_1 \hat{\delta}(t) - 2 \operatorname{sgn}(r) \delta_0]}_{\text{term2}} \\ &\quad + \underbrace{\tanh^2(k_1 r) \{ [\delta(t) - \hat{\delta}(t)]^2 - 4\delta_0^2 \}}_{\text{term3}} \end{aligned} \quad (18)$$

There are three terms in \dot{V} . Because $[\delta(t) - \hat{\delta}(t)] \in [-2\delta_0, 2\delta_0]$, term3 is always non-positive obviously. Next, term2 is examined:

Case 1: $r > 0$. The following expression is obtained:

$$\begin{cases} \tanh(k_1 r) > 0 \\ \delta(t) - \hat{\delta}(t) - 2\delta_0 \leq 0 \end{cases} \quad (19)$$

In this case, $\text{term 2} \leq 0$ is established.

Case 2: $r < 0$. The following expression is obtained:

$$\begin{cases} \tanh(k_1 r) < 0 \\ \delta(t) - \hat{\delta}(t) + 2\delta_0 \geq 0 \end{cases} \quad (20)$$

In this case, $\text{term 2} \leq 0$ is also established.

Case 3: $r = 0$.

In this case, $term\ 2 = 0$ is obviously.

Thus, sufficient condition that makes \dot{V} always negative or zero can be adjusted into the following expression:

$$\dot{V} \leq \left[-\frac{k_2}{c_1} + \frac{(\alpha - c_2)r}{c_1 \tanh(k_1 r)} \right] \tanh^2(k_1 r) - e \tanh(k_1 r) \underbrace{\left[\frac{\alpha(\alpha - c_2)}{c_1} - \frac{r}{\tanh(k_1 r)} \right]}_{term1} - \alpha e^2 \quad (21)$$

To simplify writing, the control gains k_3 and k_4 are defined as:

$$k_3 = \frac{\alpha - c_2}{c_1}, k_4 = \frac{k_2}{c_1} \quad (22)$$

Accordingly, (21) can be rewritten as follows:

$$\dot{V} \leq \left[-k_4 + \frac{k_3 r}{\tanh(k_1 r)} \right] \tanh^2(k_1 r) - e \tanh(k_1 r) \left[k_3 \alpha - \frac{r}{\tanh(k_1 r)} \right] - \alpha e^2 \quad (23)$$

In order to complete the stability analysis, two cases, when $r(t) = 0$ or $r(t) \neq 0$, are also examined.

Case 1: $r(t) = 0$. Based on the fact of $r(t) = 0$, the following expression is obtained:

$$\tanh(k_1 r) = 0 \quad (24)$$

Thus, (23) can be simplified into the following form:

$$\dot{V} = -\alpha e^2 \leq 0 \quad (25)$$

Case 2: $r(t) \neq 0$. Since $r(t) \neq 0$, the following condition exists:

$$\tanh(k_1 r) \neq 0 \quad (26)$$

At this time, (23) can be rewritten in the following manner:

$$\dot{V} = -[e \tanh(k_1 r)] M [e \tanh(k_1 r)]^T - \frac{1}{2} \alpha e^2 \quad (27)$$

where $M \in \mathbb{R}^{2 \times 2}$ is defined in the following manner:

$$M = \begin{pmatrix} \frac{\alpha}{2} & \frac{k_3}{2} \alpha - \frac{r}{2 \tanh(k_1 r)} \\ \frac{k_3}{2} \alpha - \frac{r}{2 \tanh(k_1 r)} & k_4 - \frac{k_3 r}{\tanh(k_1 r)} \end{pmatrix} \quad (28)$$

In order to ensure \dot{V} is always negative or zero, the control gains must be selected in a fashion such that the matrix M of (28) is positive definite. Thus, the control gains must be selected to guarantee that the following conditions are satisfied:

$$\frac{\alpha}{2} > 0 \quad \text{Condition (I)}$$

$|M| > 0$, that is :

$$\frac{\alpha}{2} \left(k_4 - \frac{k_3 r}{\tanh(k_1 r)} \right) - \left[\frac{k_3}{2} \alpha - \frac{r}{2 \tanh(k_1 r)} \right]^2 > 0 \quad \text{Condition (II)}$$

In order to satisfy Condition (I), $\alpha > 0$ is needed. This condition has been met in (8). Next, Condition (II) is mainly studied. Condition (II) can be re-organized into the following form:

$$\frac{\alpha}{2} k_4 - \frac{k_3^2}{4} \alpha^2 - \frac{r^2}{4 \tanh^2(k_1 r)} > 0 \quad (29)$$

After utilizing the fact in (Dixon et al., 1999; Feemster et al., 2006), the following inequality is used:

$$|r| + \frac{1}{k_1} \geq \left| \frac{r}{\tanh(k_1 r)} \right| \quad (30)$$

Therefore, condition (29) can be strengthened to (31).

$$\frac{\alpha}{2} k_4 - \frac{k_3^2}{4} \alpha^2 > \frac{1}{4} \left(|r| + \frac{1}{k_1} \right)^2 \quad (31)$$

Then, another inequality can be obtained by the Lyapunov function (17):

$$V(t) \geq \frac{1}{k_1 c_1} \ln(\cosh(k_1 r)) \geq \left(\frac{1}{c_1} |r| - \frac{1}{k_1 c_1} \ln 2 \right) \quad (32)$$

By inequality (32), the following inequality is obtained:

$$c_1 V(t) + \frac{1}{k_1} \ln 2 \geq |r| \quad (33)$$

After substituting (33) into (31), the condition can be further strengthened to (34).

$$2\alpha k_4 - k_3^2 \alpha^2 > \left(c_1 V(t) + \frac{1}{k_1} \ln 2 + \frac{1}{k_1} \right)^2 \quad (34)$$

As long as inequality (34) and $\alpha > 0$ are satisfied at the same time, $\dot{V} < 0$ holds. That is, $V(t)$ is a monotonically decreasing

function. At this time, $V(0)$ is the maximum value of $V(t)$ in the whole control process.

Accordingly, the sufficient condition of $\dot{V} < 0$ can be obtained:

$$2\alpha k_4 - k_3^2 \alpha^2 > (c_1 V(0) + \frac{1}{k_1} \ln 2 + \frac{1}{k_1})^2 \quad (35)$$

Next, the condition $V(0)$ will be analyzed and its analytical expressions can be given. When $t = 0$, the Lyapunov function (17) can be organized into the following form:

$$\begin{aligned} V(0) &= \frac{1}{k_1 c_1} \ln[\cosh(k_1 r(0))] + \frac{1}{2} e(0)^2 \\ &\leq \frac{1}{k_1 c_1} [k_1 |r(0)|] + \frac{1}{2} e(0)^2 \\ &= \frac{1}{c_1} |r(0)| + \frac{1}{2} e(0)^2 \\ &\leq \frac{1}{c_1} [|\dot{e}(0)| + \alpha |e(0)|] + \frac{1}{2} e(0)^2 \end{aligned} \quad (36)$$

Namely,

$$c_1 V(0) \leq |\dot{e}(0)| + \alpha |e(0)| + \frac{1}{2} c_1 e(0)^2 \quad (37)$$

Accordingly, with conditions (35) and (37), the following inequality is obtained:

$$\begin{aligned} 2\alpha k_4 - k_3^2 \alpha^2 &> [|\dot{e}(0)| + \alpha |e(0)| \\ &+ \frac{1}{2} c_1 e(0)^2 + \frac{1}{k_1} (1 + \ln 2)]^2 \end{aligned} \quad (38)$$

After substituting $k_3 = \frac{\alpha - c_2}{c_1}$, $k_4 = \frac{k_2}{c_1}$ into (38), the following final expression of sufficient condition that makes $\dot{V} \leq -\frac{1}{2} \alpha e^2$ established is obtained:

$$\begin{aligned} 2\alpha \frac{k_2}{c_1} - \left[\frac{\alpha - c_2}{c_1} \right]^2 \alpha^2 &> [|\dot{e}(0)| + \alpha |e(0)| \\ &+ \frac{1}{2} c_1 |e(0)|^2 + \frac{1}{k_1} (1 + \ln 2)]^2 \end{aligned}$$

Remark 5: As long as the disturbance force $\delta(t)$ or internal parameters' perturbation is bounded, the control input u (10) meeting constraint (15) can ensure that the closed-loop system is asymptotically stabilizing. Here, only the ranges of control gains have been given. The analytical approach

about how to select exact values of k_1 and k_2 isn't given here.

The optimal k_1 and k_2 need to be adjusted according to the simulation or actual test results.

5. SIMULATION RESULTS

In order to validate the performance of saturated controller, a quadrotor is selected and its parameters are measured and calculated as $l = 0.197m$, $\eta_1 = 0.05$ and $I_y = 0.0852kg \cdot m^2$.

Accordingly, the values of c_1 and c_2 in (5) are as following:

$$c_1 = 2.31, c_2 = 0.116 \quad (39)$$

The values of control gains that make the system achieve satisfactory tracking performance are selected according to (15):

$$\alpha = 5.3, k_1 = 2.0, k_2 = 70.0 \quad (40)$$

Experiment 1: The experiment of disturbance rejection

The desired pitch angle is set to a constant $\theta_d = +30^\circ$. The initial pitch angle and angular velocity signals in system (5) are given by:

$$\theta(0) = +5.0^\circ, \dot{\theta}(0) = 0^\circ / \text{sec} \quad (41)$$

Assume in the regulation process, there is a time-varying disturbance force with the following form:

$$\delta(t) = \begin{cases} 3.0 \sin(10t) & N & t \in [0, 3] \\ 2.0 & N & t \in (3, 4] \\ 1.0 & N & t \in (4, 5] \\ 0.0 & N & t \in (5, 6] \end{cases} \quad (42)$$

The maximum disturbance force that the quadrotor UAV can withstand in pitch channel is set to 2N, in the sense that $\delta_0 = 2$. The simulation process lasts for 6 seconds. The regulation effect is shown in Fig.3. The trajectory of tracking error is shown in Fig.4. The control force input u and the disturbance estimation $\hat{\delta}(t)$ are shown in Fig.5 and Fig.6.

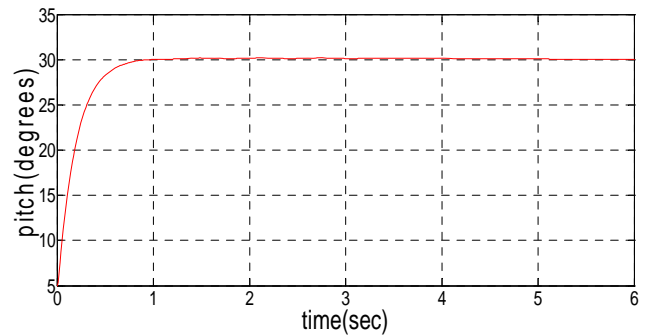


Fig. 3. Regulation effect under a time-varying disturbance.

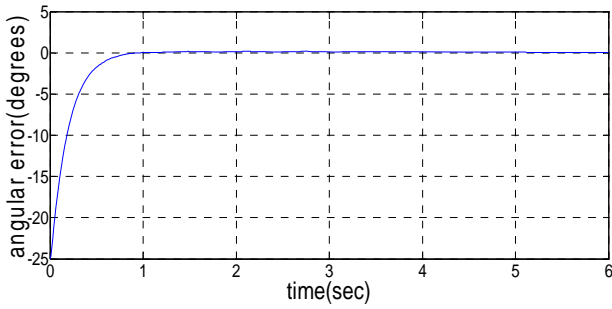


Fig. 4. Tracking error $e(t)$ under a time-varying disturbance.

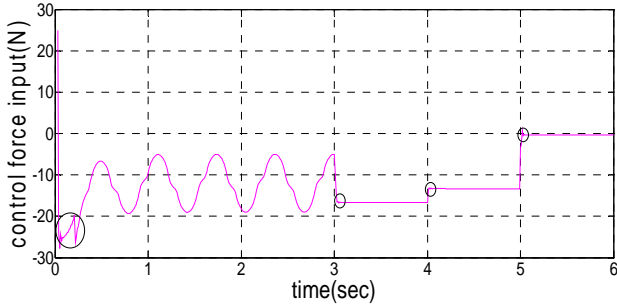


Fig. 5. Control force input . u

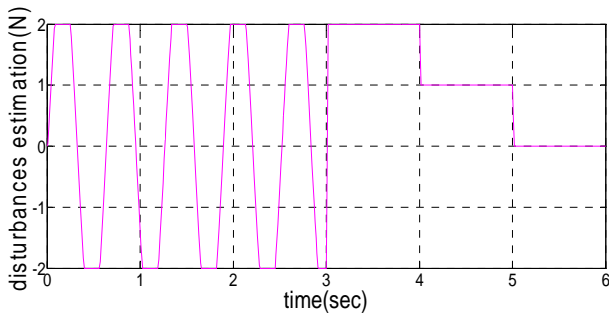


Fig. 6. Disturbances estimation $\hat{\delta}(t)$.

Experiment 2: The experiment of parameters' perturbation

The desired pitch angle, initial pitch angle and angular velocity signals remain the same as Experiment 1.

Assume in the regulation process, there is a 10% parameters' perturbation and no external disturbances in system (5). That is:

$$c_1 = 2.54, c_2 = 0.128 \tag{43}$$

$$\delta(t) = 0.0 \text{ N} \tag{44}$$

The simulation process also lasts for 6 seconds. The regulation effect is shown in Fig.7. The trajectory of error is shown in Fig.8. The control input u and the disturbance estimation $\hat{\delta}(t)$ are shown in Fig.9 and Fig.10 respectively.

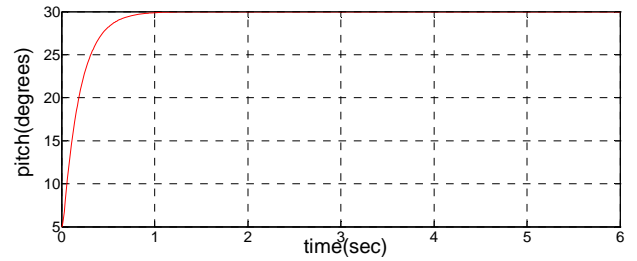


Fig. 7. Regulation effect under parameters' perturbation.

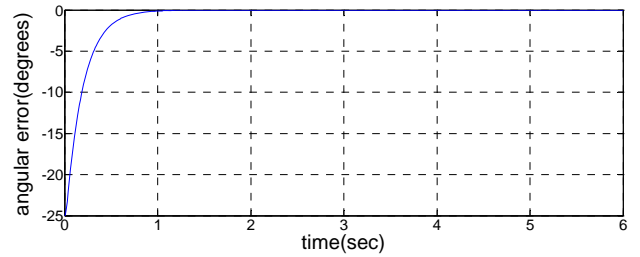


Fig. 8. Tracking error $e(t)$ under parameters' perturbation.

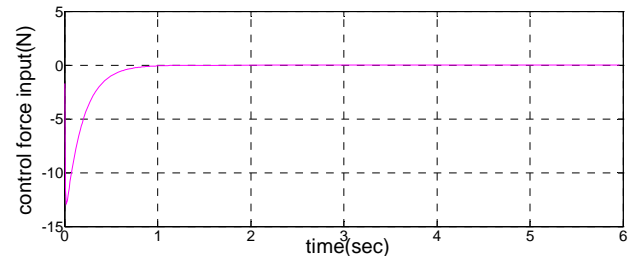


Fig. 9. Control force input u .

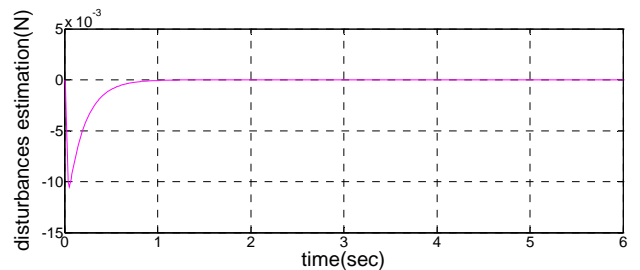


Fig. 10. Disturbances estimation $\hat{\delta}(t)$.

Experiment 3: The comprehensive experiment

$\theta(0)$ and $\dot{\theta}(0)$ remain the same as (36), $\theta_d = +30^\circ$.

Assume in the regulation process, there is an external disturbance as shown in (42) and parameters' perturbation as shown in (43) at the same time.

The regulation effect is shown in Fig.11. The trajectory of tracking error is shown in Fig.12. The control force input u and the disturbance estimation $\hat{\delta}(t)$ are shown in Fig.13 and Fig.14 respectively.

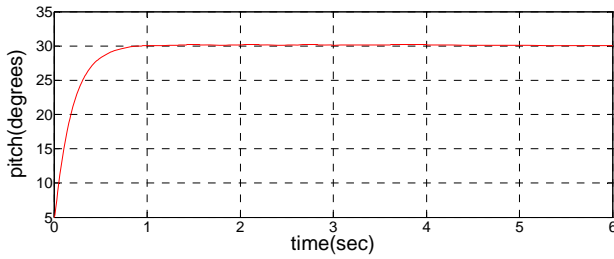


Fig. 11. Regulation effect under a complex disturbance.

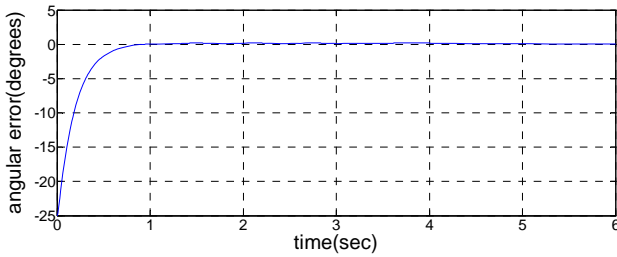


Fig. 12. Tracking error $e(t)$ under a complex disturbance.

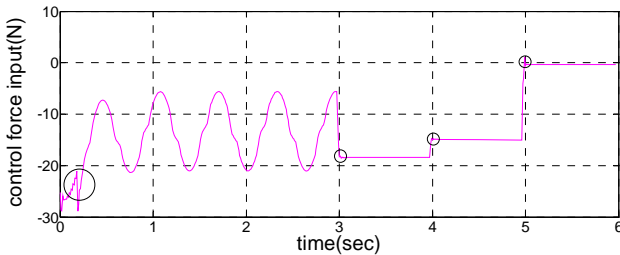


Fig. 13. Control force input u .

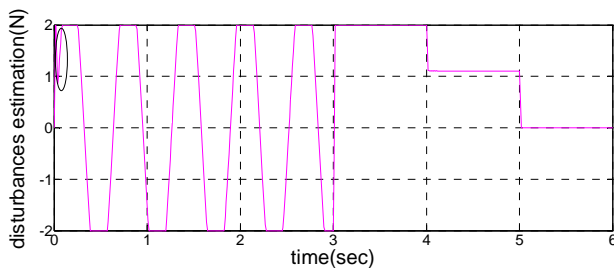


Fig. 14. Disturbances estimation $\hat{\delta}(t)$.

From Fig.3 to Fig.14, the following analysis can be made:

1) The anti-jamming performance of controller is satisfactory. When there is a sinusoidal disturbance whose

amplitude is equal to 3N, the disturbance estimation $\hat{\delta}(t)$ will enter saturated zone (see Fig.6). In this case, there is an estimation error. But the closed-loop system is still asymptotically stabilizing under the control force input u (see Fig.3) and there is no steady-state error. Moreover, the tracking error is monotonic convergence (see Fig.4). In addition, when the disturbance just appears or switches, the control force input u has small amplitude fluctuations. This phenomenon is reasonable and is in controllable range (see Fig.5).

2) The anti-parameters' perturbation performance of the controller is excellent. When the parameters' perturbation is up to 10% amplitude and there is no disturbance, the amplitude of disturbance estimation is very small (the maximum value is approximately equal to $|-10 \times 10^{-3}| = 0.01$, see Fig.10). This shows that the disturbance estimation algorithm is reliable. The regulation effect, tracking error $e(t)$ and control force input u all have a smooth transition. Their dynamic process is satisfactory (see Fig.7, Fig.8 and Fig.9). In addition, from simulation results, parameters' perturbation has a smaller impact on the regulation process than external disturbances (see Fig.3, Fig.7, Fig.5 and Fig.9).

3) When the external disturbance and internal parameters' perturbation exist simultaneously, the control input u is still able to guarantee the closed-loop system is asymptotically stabilizing (see Fig.11 and Fig.12). In the initial appearance of disturbance (it lasts for about 0.3 seconds, see Fig.13 and

Fig.14), the control input u and disturbance estimation $\hat{\delta}(t)$ have some jitter but not much. After that, the smooth control input and stabilizing track of external disturbance can be achieved. The slight jitter of control input u in the 3rd, 4th and 5th seconds is due to the sudden switch of the external disturbance (see Fig.13).

6. CONCLUSIONS

A nonlinear saturated attitude controller to stabilize a quadrotor UAV has been presented. Satisfactory simulation results have been achieved. The most important contribution of this paper is to propose a novel control strategy that is not sensitive to unknown disturbances' structure and parameters' perturbation. The saturated controller obtained via a Lyapunov function is useful to achieve asymptotic stability in the case with the presence of various typical kinds of unknown disturbances and parameters' perturbation.

Future work will be focused on the expansion of the controller so that not only attitude but also other elements of translational motion, i.e. position and velocity are collectively controlled by this nonlinear saturated force controller.

ACKNOWLEDGEMENTS

This work was financially supported by the National Natural Science Foundation of China (NO. U1433103) to Runxia Guo and the Basic R&D Operating Expenses of CAUC with No. 3122014B002, No. 3122014D022 and No. 3122013x003. The authors would like to express gratitude.

The authors would also like to thank the reviewers for their fair comments on improving the paper.

REFERENCES

Abdolhosseini, M., Zhang, Y.M., and Rabbath C.A. (2012). Explicit MPC for LPV Systems: Stability and Optimality. *IEEE Trans. Automatic Control*. 52(9):2322–2332.

Abdolhosseini, M., Zhang, Y.M., and Rabbath C.A. (2013). An Efficient Model Predictive Control Scheme for an Unmanned Quadrotor Helicopter. *Journal of intelligent & robotic systems*. 70(1-4):27–38.

- Dixon, W.E., de Queiroz, M.S., Zhang, F., Dawson, D.M. (1999). Tracking Control of Robot Manipulators with Bounded Torque Inputs. *Robotica*. 17:121–129.
- Feemster, M.G., Fang, Y.C., and Dawson, D.M. (2006). Disturbance Rejection for a Magnetic Levitation System. *IEEE Trans. Mechatronics Technology*. 11(6):709–717.
- Khebbache, H., Tadjine, M. (2013). Robust Fuzzy Backstepping Sliding Mode Controller For a Quadrotor Unmanned Aerial Vehicle. *Journal of Control Engineering and Applied Informatics*. 15(2):3–11.
- Kutay, A.T., Calise, A. J., Idan, M., and Hovakimyan, N. (2005). Experimental Results on Adaptive Output Feedback Control Using a Laboratory Model Helicopter. *IEEE Trans. Control Systems Technology*. 13(2):196–202.
- Lee, T. (2013). Robust Adaptive Attitude Tracking on $SO(3)$ with an Application to a Quadrotor UAV. *IEEE Trans. Control Systems Technology*. 21(5):1924–1930.
- Nagaty, A., Saeedi, S., Thibault, C., Seto, M., and Li, H. (2013). Control and Navigation Framework for Quadrotor Helicopters. *Journal of intelligent & robotic systems*. 70(1-4):1–12.
- Santos, O., Romero, H., Salazar, S., and Lozano, R. (2013). Real-time Stabilization of a Quadrotor UAV: Nonlinear Optimal and Suboptimal Control. *Journal of intelligent & robotic systems*. 70(1-4):79–91.
- Srinivasan, B., Huguenin, P., and Bonvin, D. (2009). Global Stabilization of an Inverted Pendulum-control Strategy and Experimental Verification. *IEEE Trans. Automatic Control*. 45(1):265–269.
- Xu, R., Ozguner, U. (2008). Sliding Mode Control of a Class of Underactuated Systems. *IEEE Trans. Automatic Control*. 44(1):233–241.
- Zhang, R., Quan, Q., and Cail, K.Y. (2010). Attitude control of a quadrotor aircraft subject to a class of time-varying disturbances. *IET Control Theory and Applications*. 5(9):1140–1146.